Supporting Information

Zn(II) complexation promotes isomerization and oxidative rearrangements of naringenin: evidence from IR ion spectroscopy and DFT calculations

Lucretia Rotari,[†a] Valeria Vergine,[†a] Giel Berden,[bc] Jos Oomens,[bc] Barbara Chiavarino,*[a] Davide Corinti*[a] and Maria Elisa Crestoni[a]

[a] Dipartimento di Chimica e Tecnologie del Farmaco , Sapienza Università di Roma, Piazzale Aldo Moro 5, 00185 Rome, Italy;
[b] HFML-FELIX, Toernooiveld 7, 6525ED Nijmegen, the Netherlands
[c] Institute for Molecules and Materials, Radboud University, Heyendaalseweg 135, 6525AJ Nijmegen, the Netherlands

† These authors contributed equally to this work.
*** Corresponding authors**

Table of Contents

Fig. S1. ESI mass spectrum of the naringenin- $ZnSO_4$ solution.

Fig. S2. CID spectrum of $[Zn(Nar-H)]^+$ (blu trace) compared to the CID spectrum of $[Zn(ChNar-H)]^+$ (orange trace) both recorded at CE of 17 V.

Table S1. Main fragment ions observed in the CID spectra of $[Zn(Nar-H)]^+$ and $[[Zn(ChNar-H)]^+$ complexes

Fig. S3. IRMPD spectrum of $[Zn(Nar-H)]^+$ in blue, compared to that of $[Zn(ChNar-H)]^+$ displayed as a faded red profile.

Fig. S4. IRMPD spectrum of $[Zn(Nar-H)]^+$ (blue profile) compared to the calculated IR spectra (black profiles) of selected isomers at the B3LYP level with their optimized geometries. Relative enthalpies (free energies) at 298 K are reported in kJ mol^{-1}.

Table S2. Thermodynamic data at 298K calculated for selected $[Zn(Nar-H)]^+$ isomers and conformers.

Table S3. Experimental IRMPD bands of $[Zn(Nar-H)]^+$ compared to calculated vibrational modes **NarZn_1** Band positions are reported in cm^{-1}, while calculated intensities (Int) are in km mol^{-1}.

Figure S5. Fragmentation spectra of A) $[Api+H]^+$, B) $[Geni+H]^+$ and C) $[Nar-H]^+$ generated by dissociation of $[Zn(Nar-H)]^+$.

Fig. S6. IRMPD spectrum of $[Api+H]^+$ (green profile) compared to the calculated IR spectra (black profiles) of higher energy isomers showing protonation on the C3 or C2 atoms.

Fig. S7. IRMPD spectrum of $[Api+H]^+$ (green profile) compared to the calculated IR spectra (black profiles) of the four lowest lying conformers of apigenin protonated on the carbonyl oxygen (C4=O), with anticlockwise orientation of both hydrogen atoms in 5-OH and 4-OH position.

Fig. S8. IRMPD spectrum of $[Api+H]^+$ (green profile) compared to the calculated IR spectra (black profiles) of the four lowest lying conformers of apigenin protonated on the carbonyl oxygen (C4=O), with clockwise orientation of both hydrogen atoms in 5-OH and 4-OH position.

Fig. S9. IRMPD spectrum of $[Geni+H]^+$ (red profile) compared to the calculated IR spectra (black profiles) of the four lowest lying conformers of genistein protonated on the carbonyl oxygen (C4=O), with anticlockwise orientation of both hydrogen atoms in 5-OH and 4-OH position.

Fig. S10. IRMPD spectrum of $[Geni+H]^+$ (red profile) compared to the calculated IR spectra (black profiles) of the four lowest lying conformers of genistein protonated on the carbonyl oxygen (C4=O), with clockwise orientation of both hydrogen atoms in 5-OH and 4-OH position.

Table S4. Experimental IRMPD bands of $[Api+]^+$ compared to calculated vibrational modes **ApiH_1**. Band positions are reported in cm^{-1}, while calculated intensities (Int) are in km mol^{-1}.

Table S5. Experimental IRMPD bands of $[Geni+H]^+$ compared to calculated vibrational modes **GenH_1**. Band positions are reported in cm^{-1}, while calculated intensities (Int) are in km mol^{-1}.

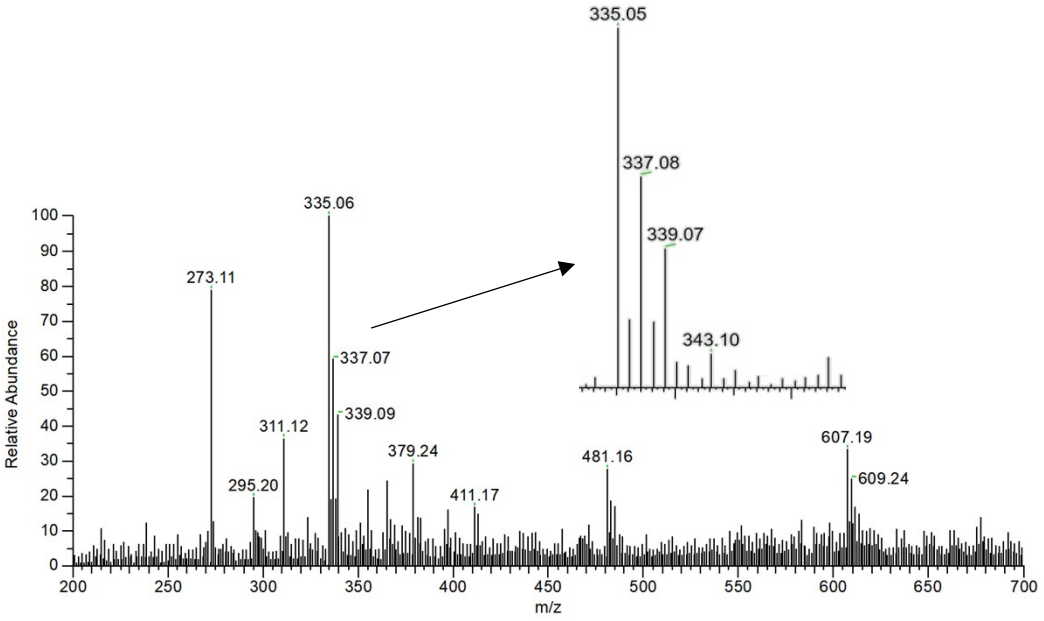

Fig. S1. ESI mass spectrum of the naringenin-$ZnSO_4$ solution.

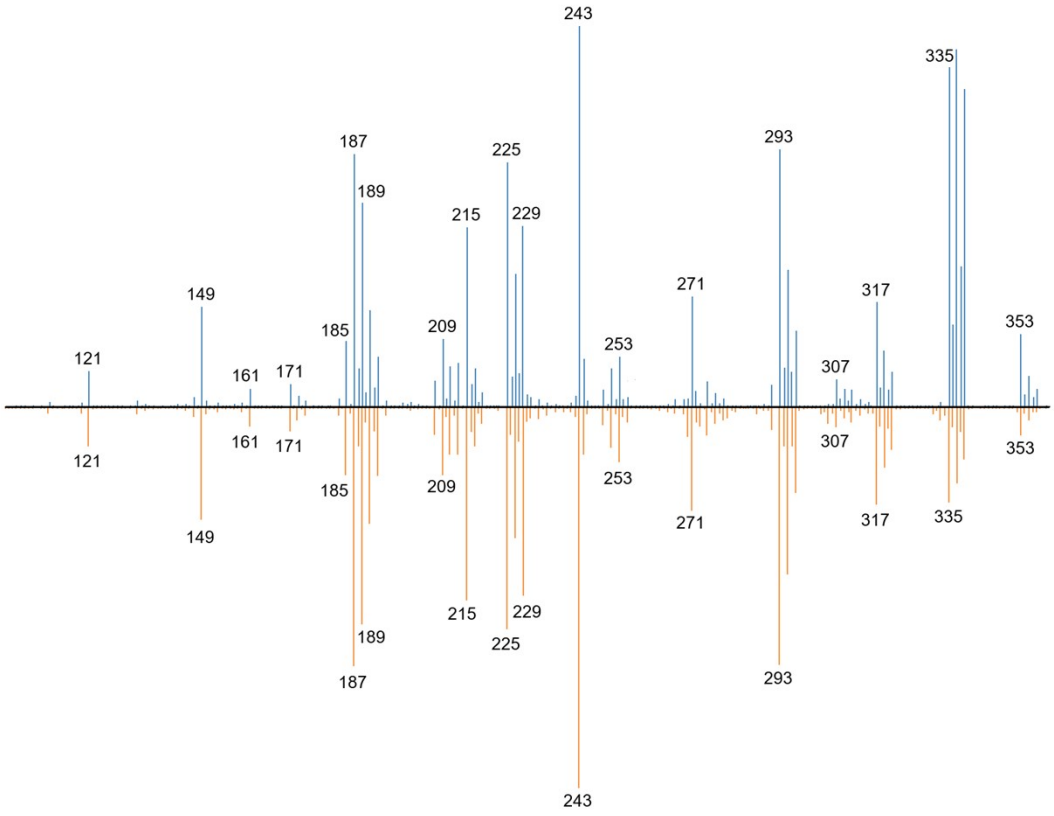

Fig. S2. CID spectrum of $[Zn(Nar-H)]^+$ (blu trace) compared to the CID spectrum of $[Zn(ChNar-H)]^+$ (orange trace) both recorded at CE of 17 V.

Table S1. Main fragment ions observed in the CID spectra of $[Zn(Nar-H)]^+$ and $[Zn(ChNar-H)]^+$ complexes

Fragments ion (m/z)	Neutral loss	Neutral loss attributions
317	18	$-H_2O$
307	28	-CO
293	42	$-C_2H_2O$
271	64	-Zn
253	82	-2CO $-H_2O$
243	92	-Zn -CO
225	110	-2CO $-3H_2O$
229	106	-Zn $-C_2H_2O$
215	120	-Zn -2CO
209	126	-1,3,5 trihydroxylbenzene
189	146	$-C_9H_6O_2$
187	148	-Zn -3CO
185	150	-Zn - C_2H_2O $-C_2H_2$ $-H_2O$
161	174	-Zn -2CO $-3H_2O$
149	186	-Zn $-C_8H_{10}O$

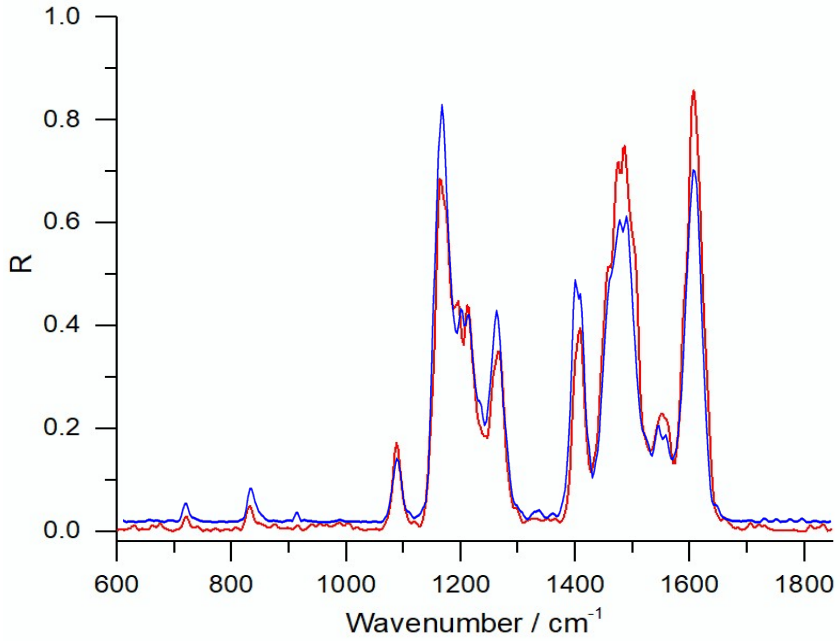

Fig. S3. IRMPD spectrum of $[Zn(ChNar-H)]^+$ in red, compared to that of $[Zn(Nar-H)]^+$ displayed as a faded blue profile.

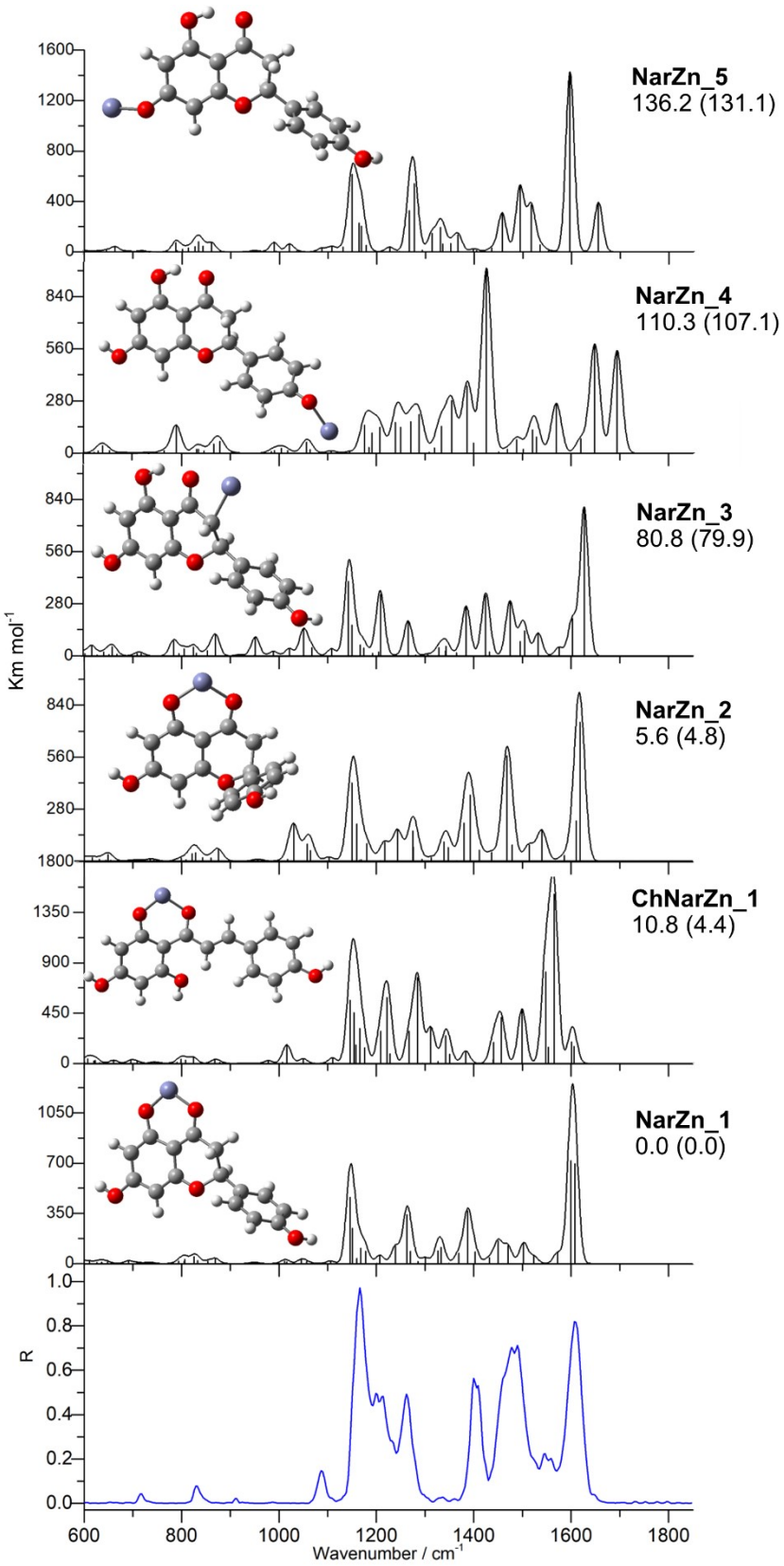

Fig. S4. IRMPD spectrum of $[Zn(Nar{-}H)]^+$ (blue profile) compared to the calculated IR spectra (black profiles) of selected isomers at the B3LYP level with their optimized geometries. Relative enthalpies (free energies) at 298 K are reported in kJ mol^{-1}.

Table S2. Thermodynamic data at 298K calculated for selected $[Zn(Nar-H)]^{+}$ $^{+}$ isomers and conformers.

	B3LYP-D3/6-311++G(d,p)				B2PLYP/def2TZVP			
	H corrected EE[a]	G corrected EE[a]	rel H[b]	rel G[b]	H corrected EE[a]	G corrected EE[a]	rel H[b]	rel G[b]
NarZn_1	-2733.495271	-2733.560703	0.00	0.00	-2732.583695	-2732.648919	0.00	0.00
ChNarZn_1	-2733.491145	-2733.559027	10.83	4.40	-2732.576146	-2732.643882	19.82	13.22
NarZn_2	-2733.493125	-2733.558882	5.63	4.78	-2732.580663	-2732.641673	7.96	19.02
NarZn_3	-2733.464487	-2733.530265	80.82	79.91				
NarZn_4	-2733.453254	-2733.519925	110.32	107.06				
NarZn_5	-2733.443387	-2733.510755	136.22	131.14				

[a] in Hartree/particle; [b] in kJ/mol

Table S3. Experimental IRMPD bands of $[Zn(Nar-H)]^{+}$ compared to calculated vibrational modes **NarZn_1**. Band positions are reported in cm^{-1}, while calculated intensities (Int) are in km mol^{-1}.

Exp	**NarZn_1**		**Vibrational assignment**
	Freq	**Int**	
1608 (intense)	1625	748	C7-O7, C6-C8a and C6-C5 stretchings
	1617	216	C4'-O, C5'-C6' and C3'-C2' stretchings
1549 (small)	1546	165	C8-C7-C6 asymm stretching + O7-H bending
	1520	88	ring B C-H bending ip
1482 (intense)	1485	86	C4a-C4, C7-O7 stretching
	1474	567	C4-O and C5-O stretchings, C6-H and C8-H bendings
1405 (medium)	1398	356	C3-H_2 scissoring, C4-O stretching
	1386	205	C3-H_2 wagging, C2-H bending
1334 (very small)	1352	74	O4'-H bending ip, C2-H bending
	1344	102	C2-H bending, C4'-O4' bending ip
1262 (medium)	1280	162	C4'-O4' stretching, ring B CH bending ip
	1248	166	C3-H2 wagging, C2-H bending
1206 (shoulder)	1222	100	O7-H bending, C3-H_2 twisting
	1185	93	C3-H_2 twisting, C6-H bending
1168 (most intense)	1164	200	O4'-H bending ip
	1154	422	O7-H bending, C8-H bending
1085 (small)	1062	92	C2-C3, C4a-C8a stretching
	1034	197	ring C breathing
830 (small)	878	61	C2-O1 stretching
	832	45	ring B CH bendings oop
715 (very small)	670	34	O5-Zn-O4 asymm stretching, ring A breathing

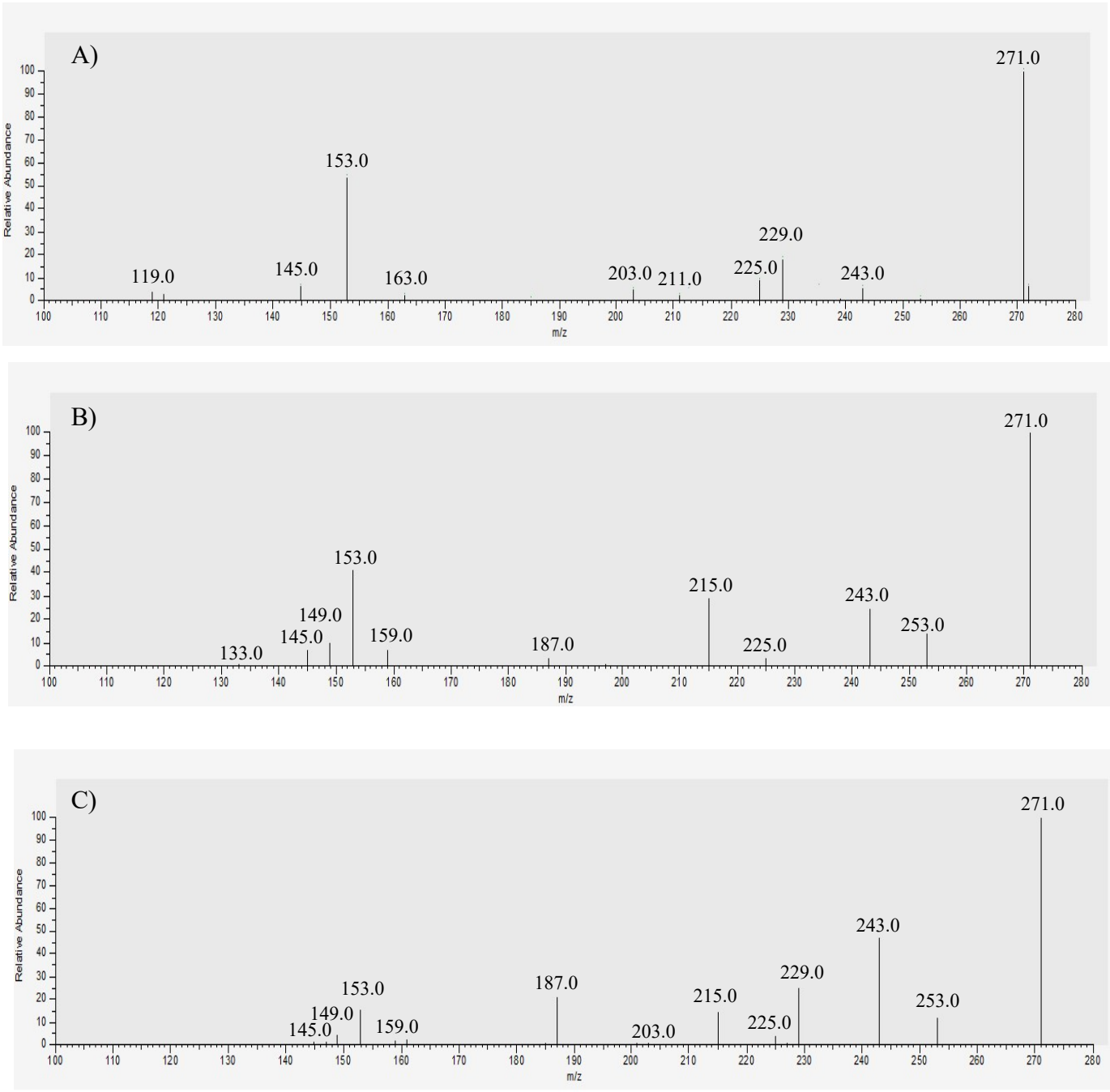

Fig. S5. Fragmentation spectra of A) $[Api+H]^+$, B) $[Geni+H]^+$ and C) $[Nar-H]^+$ generated by dissociation of $[Zn(Nar-H)]^+$.

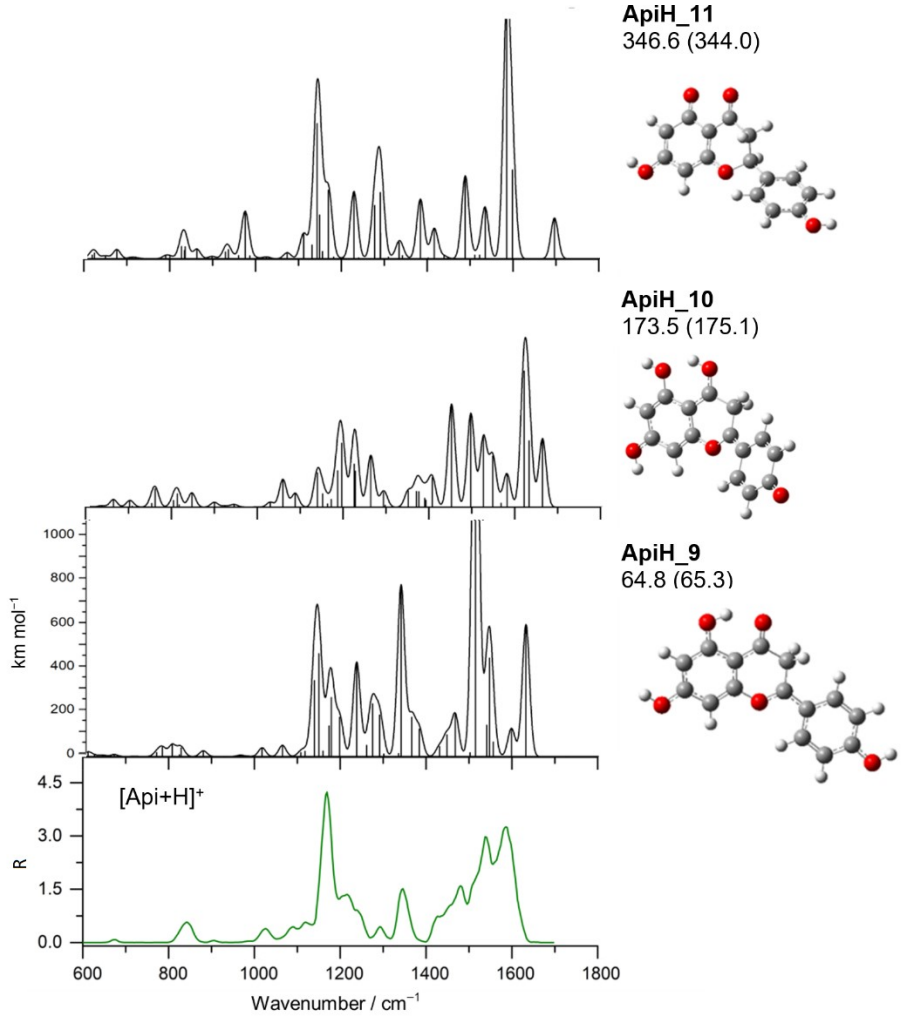

Fig. S6. IRMPD spectrum of $[Api+H]^+$ (green profile) compared to the calculated IR spectra (black profiles) of higher energy isomers showing protonation on the C3 or C2 atoms. Optimized structures are reported on the right. Relative enthalpies (free energies), respect to the global minimum **ApiH_1** at 298 K are reported in kJ mol^{-1}. Absolute intensities in km mol^{-1} are the same for all calculated IR spectra.

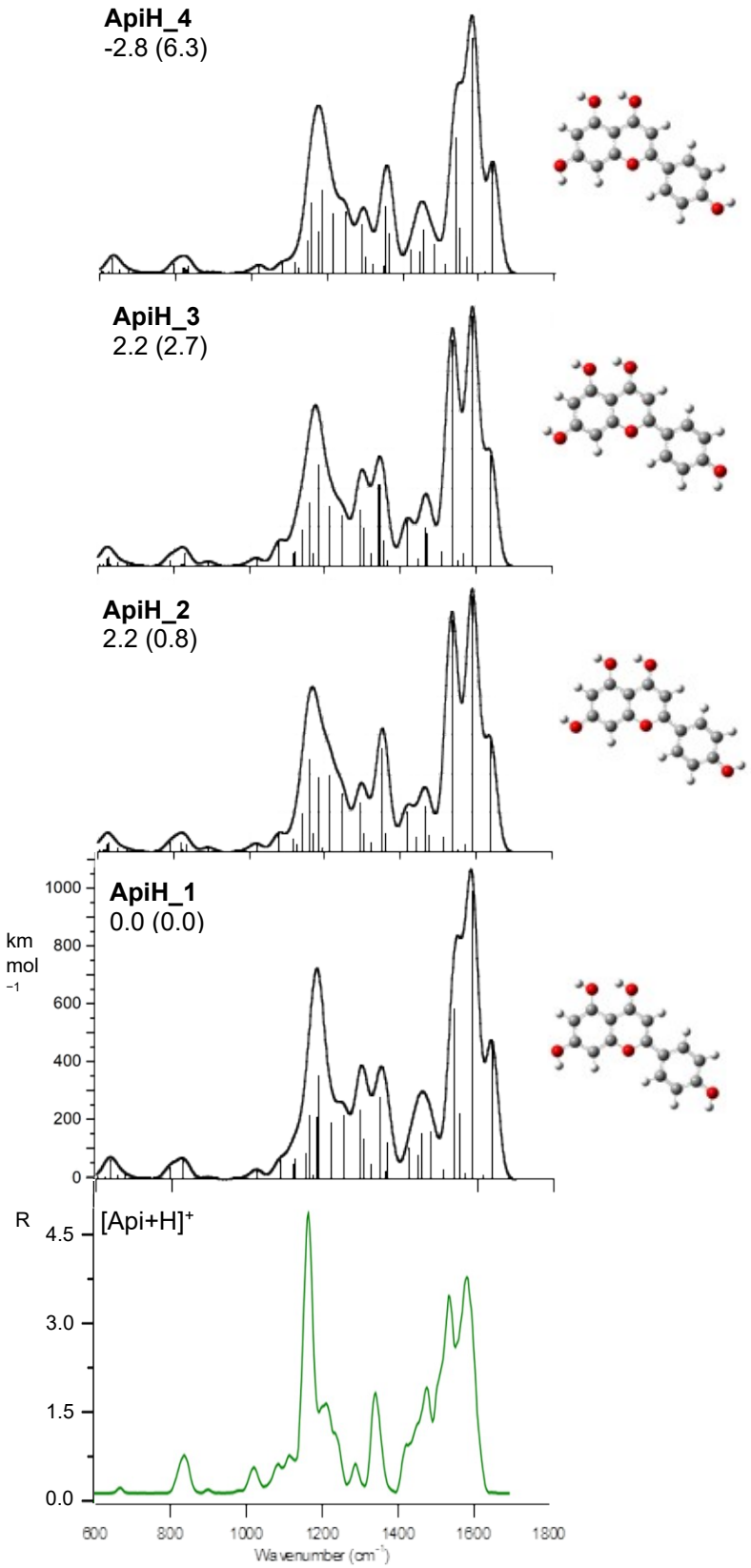

Fig. S7. IRMPD spectrum of $[Api+H]^+$ (green profile) compared to the calculated IR spectra (black profiles) of the four lowest lying conformers of apigenin protonated on the carbonyl oxygen (C4=O), with anticlockwise orientation of both hydrogen atoms in 5-OH and 4-OH position. Optimized structures are reported on the right. Relative free energies at 298 K are reported in kJ mol^{-1}. Absolute intensities in km mol^{-1} are the same for all calculated IR spectra.

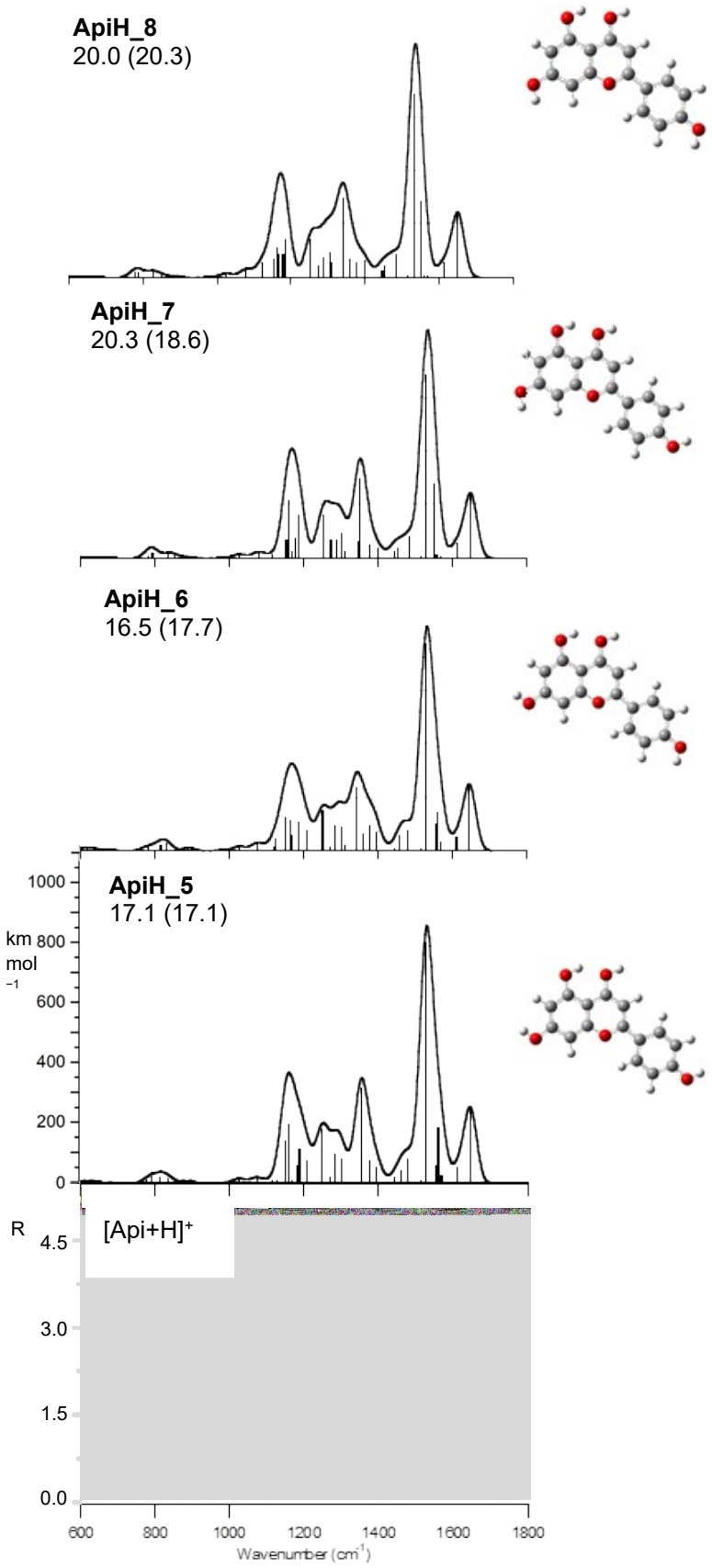

Fig. S8. IRMPD spectrum of $[Api+H]^+$ (green profile) compared to the calculated IR spectra (black profiles) of the four lowest lying conformers of apigenin protonated on the carbonyl oxygen (C4=O), with clockwise orientation of both hydrogen atoms in 5-OH and 4-OH position. Optimized structures are reported on the right. Relative free energies (respect to **ApiH_1)** at 298 K are reported in kJ mol^{-1}. Absolute intensities in km mol^{-1} are the same for all calculated IR spectra.

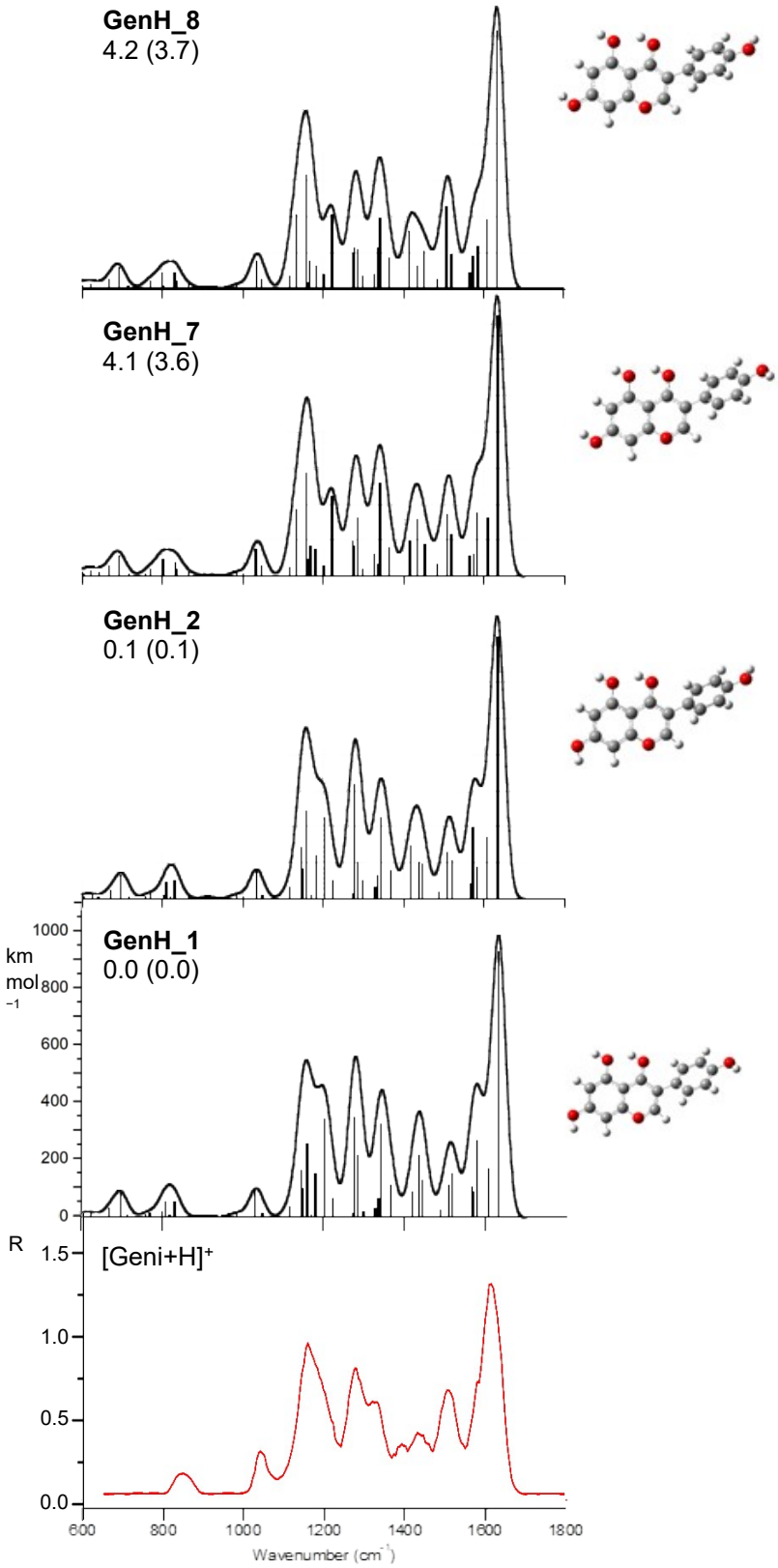

Fig. S9. IRMPD spectrum of $[Geni+H]^+$ (red profile) compared to the calculated IR spectra (black profiles) of the four lowest lying conformers of genistein protonated on the carbonyl oxygen (C4=O), with anticlockwise orientation of both hydrogen atoms in 5-OH and 4-OH position. Optimized structures are reported on the right. Relative free energies at 298 K are reported in kJ mol^{-1}. Absolute intensities in km mol^{-1} are the same for all calculated IR spectra.

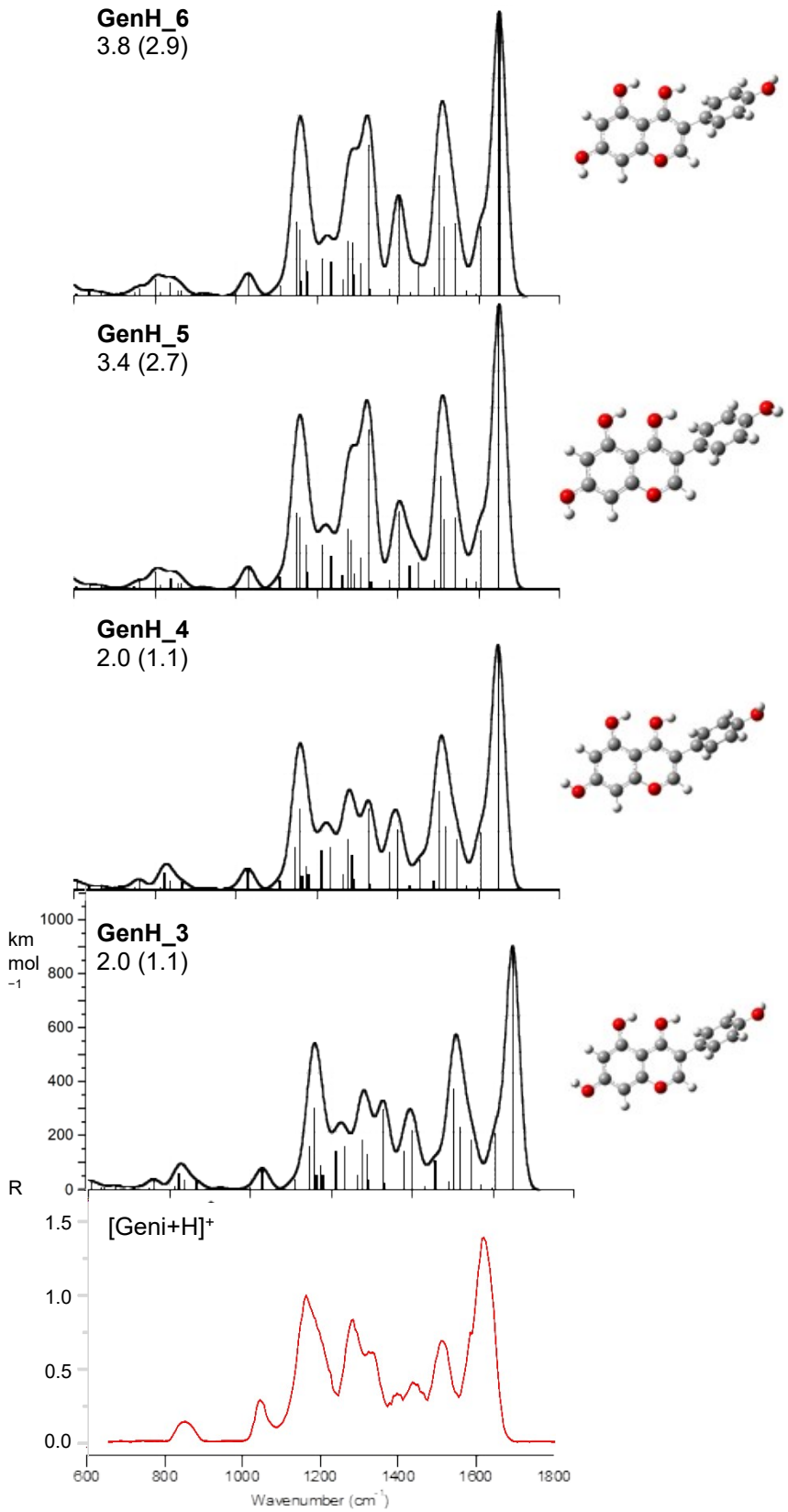

Fig. S10. IRMPD spectrum of $[Geni+H]^+$ (red profile) compared to the calculated IR spectra (black profiles) of the four lowest lying conformers of genistein protonated on the carbonyl oxygen (C4=O), with clockwise orientation of both hydrogen atoms in 5-OH and 4-OH position. Optimized structures are reported on the right. Relative free energies at 298 K are reported in kJ mol^{-1} respect to the global miminum **GenH_1**. Absolute intensities in km mol^{-1} are the same for all calculated IR spectra.

Table S4. Experimental IRMPD bands of $[Api+H]^+$ compared to calculated vibrational modes **ApiH_1**. Band positions are reported in cm^{-1}, while calculated intensities (Int) are in km mol^{-1}.

Exp	**ApiH_1**		**Vibrational assignment**	
$[Api+H]^+$	**Freq**	**Int**		
1589	1638	583	stretching CC (ring A and C) + bending CH (ring A and C) ip	
	1589	1309	stretching CC + bending H ip	
1537	1556	302	stretching CC + bending H (C3 and C2') ip + bending H ip	
	1545	724	stretching CC (ring A and C) + bending OH (C4 and C7) ip	
1480	1481	200	stretching CC + bending H (C3 and C8) ip + bending CH (ring B) ip	
	1455	175	stretching CC + bending H (C6) ip + bending H (ring B) ip	
1430	1444	82	stretching CC + stretching C4O	
	1427	172	stretching C4-OH + stretching CC + bending CH ip	
1340	1381	100	stretching CC (ring A) + bending OH ip	
	1351	382	bending H (ring B) ip + bending OH (C4 and C5) ip + stretching CC (ring A and B)	
	1324	83	bending OH (C4) ip + bending H (ring B) ip	
1294	1302	236	stretching C4'-OH + bending H (ring B) ip	
	1295	218	bending OH (C4 and C5) ip + bending H (C3 and C2') ip	
1240	1246	278	stretching C5-OH + bending CH ip	
1216	1215	298	bending H (C3) ip + bending OH (C4 and C7) ip + stretching C4-OH	
1170	1181	246	bending H ip	
	1174	145	bending OH (C5) ip + bending OH (C7) ip + bending H (ring B) ip	
	1161	442	bending H (ring B) ip	
	1151	165	bending H (ring A) ip	
1120	1115	65	bending H (ring B) ip	
	1112	63	stretching CC (ring A and C) + bending H (C3) ip + bending OH (C4 and C7) ip	
1025	1079	92	stretching C5-OH + stretching CC breathing (ring A and C) + bending H ip + bending OH (ring A and C) ip	
844	832	71	bending CH oop	
677	655	70	bending OH (C4) oop	

Table S5. Experimental IRMPD bands of $[Geni+H]^+$ compared to calculated vibrational modes **GenH_1**. Band positions are reported in cm^{-1}, while calculated intensities (Int) are in km mol^{-1}.

Exp	**GenH_1**		**Vibrational assignment**
$[Geni+H]^+$	**Freq**	**Int**	
1614	1636	692	stretching CC (ring A)
1588	1606	177	stretching CC (ring B)
	1587	138	stretching CC + bending H (C2) ip
	1575	83	stretching CC (ring B) + bending H (ring B) ip
1514	1523	111	stretching CC (ring A and C) + bending OH (C4 and C7) ip
	1509	192	stretching C4'-OH + bending H (ring B) ip
1440	1456	66	stretching C5-OH + stretching CC (ring A and B) + bending H (C6) ip + bending OH (C4) ip
	1432	91	stretching C4-OH + stretching CC + bending H (ring B) ip
	1419	130	stretching C4-OH + stretching CC (ring A) + bending H ip
1397	1375	77	stretching CC (ring A) + bending OH (C5 and C7) ip + bending H (C2 and C8) ip
1329	1345	198	bending OH (C4 and C5) ip + stretching CC (ring A)
1285	1293	103	bending OH (C4) ip + bending CH (ring B) ip
	1281	181	stretching CC breathing (ring B) + stretching C4'-OH
1220	1225	210	bending CH (ring A) ip + stretching C5-OH + stretching O1-C2
1190	1166	65	bending H (ring A) ip + bending OH (C4) ip
1164	1160	397	bending OH (C4') ip + bending H (C3' and 5') ip
	1133	618	bending H (ring A) ip
1045	1032	259	stretching C5-OH + stretching CC breathing (ring A and C) + bending CH ip
856	854	38	bending CH (ring B) oop
	701	44	bending OH (C4) oop